Association between the expression levels of ADAMTS16 and BMP2 and tumor budding in hepatocellular carcinoma

DI JIANG[1*], SHAOSHAO XU[1*], CHUANPENG ZHANG[2], CHUANBING HU[3], LEI LI[4], MINGMING ZHANG[4], HAIYAN WU[5], DONGCHANG YANG[6] and YANRONG LIU[1,4]

[1]Cheeloo College of Medicine, Shandong University, Jinan, Shandong 250012; [2]Medical Research Center, Affiliated Hospital of Jining Medical University; Departments of [3]Pediatric Surgery, [4]Pathology, [5]Medical Equipment and [6]Surgery, Affiliated Hospital of Jining Medical University, Jining, Shandong 272029, P.R. China

Received November 22, 2022; Accepted March 27, 2023

DOI: 10.3892/ol.2023.13842

Abstract. Tumor budding (TB) has become a crucial factor for predicting the malignancy grade and prognostic outcome for multiple types of solid cancer. Studies have investigated the prognostic value of TB in hepatocellular carcinoma (HCC). However, its molecular mechanism in HCC remains unclear. To the best of our knowledge, the present study was the first to compare the expression of differentially expressed genes (DEGs) between TB-positive (TB-pos) and TB-negative HCC tissues. In the present study, total RNA was extracted from 40 HCC tissue specimens and then sequenced. According to Gene Ontology (GO) functional annotation, upregulated DEGs were markedly associated with embryonic kidney development-related GO terms, which suggested that the TB process may at least partly mimic the process of embryonic kidney development. Subsequently, two genes, a disintegrin and metalloproteinase domain with thrombospondin motifs 16 (ADAMTS16) and bone morphogenetic protein 2 (BMP2), were screened and verified through immunohistochemical analysis of HCC tissue microarrays. According to the immunohistochemical results, ADAMTS16 and BMP2 were upregulated in TB-pos HCC samples, and BMP2 expression was increased in budding cells compared with the tumor center. Additionally, through cell culture experiments, it was demonstrated that ADAMTS16 and BMP2 may promote TB of liver cancer, thus promoting the malignant progression of liver cancer. Further analysis revealed that ADAMTS16 expression was associated with necrosis and cholestasis, and BMP2 expression was associated with the Barcelona Clinic Liver Cancer stage and the vessels encapsulating tumor clusters. Overall, the findings of the present study provided insights into the possible mechanisms of TB in HCC and revealed potential anti-HCC therapeutic targets.

Correspondence to: Dr Dongchang Yang, Department of Surgery, Affiliated Hospital of Jining Medical University, 89 Guhuai Road, Jining, Shandong 272029, P.R. China
E-mail: dongchang0707@163.com

Professor Yanrong Liu, Cheeloo College of Medicine, Shandong University, 44 Wenhua Xi Road, Jinan, Shandong 250012, P.R. China
E-mail: liuyanrong1984@163.com

*Contributed equally

Key words: tumor budding, hepatocellular carcinoma, a metalloproteinase domain with thrombospondin motifs 16, bone morphogenetic protein 2, molecular mechanism

Introduction

According to the 2020 Global Cancer Statistics, liver cancer ranks 6th in terms of global morbidity and 3rd among causes of cancer-associated mortality worldwide (1). Hepatocellular carcinoma (HCC) is the most frequent subtype of primary liver cancer that occurs in 75-85% of patients with liver cancer (2). Despite the great progress made in anti-HCC therapy, HCC is associated with a poor prognostic outcome (3). Tumor metastasis is an important factor contributing to the poor HCC prognosis (4). Tumor budding (TB) is defined as dissociation of isolated cancer cells and/or discrete clusters (<5 cancer cells), and its prognostic role was first reported in colorectal cancer (CRC) (5). In addition to CRC, TB has been observed in various cancer types and predicts a poor prognosis, including in esophageal (6), nasopharyngeal (7), lung (8) and pancreatic cancer (9). Furthermore, TB has been reported to be associated with epithelial-mesenchymal transition (EMT), which is a critical event that supports tumor migration and invasion (10,11). However, the impact of TB on HCC remains poorly understood. Only two studies have analyzed the prognostic value of TB in HCC (12,13), while the mechanistic basis of TB in HCC remains unclear.

A disintegrin and metalloproteinase domain with thrombospondin motifs 16 (ADAMTS16) belongs to the ADAMTS family. Its role has been investigated in esophageal squamous cell carcinoma (14) and CRC (15,16). However, to the best of our knowledge, the role of ADAMTS16 in HCC has not yet been studied. Bone morphogenetic protein 2 (BMP2), which belongs to the transforming growth factor-β superfamily, participates in different cancer occurrence and development processes (17-19). Certain studies have indicated that BMP2 enhances HCC cell growth, invasion and migration (20,21).

However, the relationship between BMP2 and TB in HCC remains to be studied.

The aim of this study was to identify differentially expressed genes (DEGs) in TB-positive (TB-pos) HCC tissue samples relative to TB-negative (TB-neg) HCC tissue samples through bioinformatics analysis, and then explore the potential mechanism of TB in HCC. In the present study, it was demonstrated that ADAMTS16 and BMP2 levels were significantly increased in the TB-pos HCC samples, and BMP2 expression was significantly increased in budding cells compared with the tumor center. Additionally, it was demonstrated that overexpression (OE) of ADAMTS16 and BMP2 promoted invasion of HepG2 cells, which implied that ADAMTS16 and BMP2 may regulate TB in liver cancer. The association of ADAMTS16 and BMP2 expression with clinicopathological characteristics and patient survival time were also analyzed. The findings of the present study provide novel mechanistic insights into the role of ADAMTS16 and BMP2 in HCC.

Materials and methods

Patients and tissues. Paraffin-embedded tumor specimens from patients with HCC (n=308) were retrospectively collected from The Affiliated Hospital of Jining Medical University (Jining, China) between June 2013 and August 2019. The clinical and pathological details of the patients were retrospectively reviewed by accessing the hospital's existing electronic medical record system. Ultimately, 266/308 (86%) of patients with HCC with complete clinical information were selected for the subsequent clinical significance analysis. In addition, of the 308 patients, 66 were excluded from the survival analysis due to a lack of follow-up. And additional 40 HCC tissue samples were prospectively collected from The Affiliated Hospital of Jining Medical University between February 2020 and June 2021 for transcriptome sequencing. All samples were histopathologically and clinically confirmed as HCC tissues. The histology, diagnostic methods, and α-fetoprotein (AFP) levels were reviewed for each case of HCC identified to eliminate cases of metastatic cancer or other primary liver cancer types. Microscopically, the HCC cells were arranged in solid nests, trabeculae, acinar or pseudoglandular structures. Papillary structures were occasionally seen. Abundant sinusoidal capillaries could be seen between the tumor alveolus, with steatosis and eosinophilic bodies. Ethics approval was provided by The Ethics Committee of The Affiliated Hospital of Jining Medical University (Jining, China; ethical approval no. 2021C145). Each participant (>18 years of age) in the study provided written informed consent and signed informed consent forms.

Cell culture and lentiviral infection. The human hepatoblastoma cell line, HepG2, was purchased from ATCC via the Shanghai Huiying Biological Technology Co., Ltd. The cell line was authenticated by human STR profiling and confirmed to be mycoplasma free. HepG2 cells were cultured in DMEM (Nanjing KeyGen Biotech Co., Ltd.) containing 10% fetal bovine serum (FBS; Biological Industries) and 1% penicillin-streptomycin (Nanjing KeyGen Biotech Co., Ltd.), and incubated in a humidified 5% CO_2 incubator at 37˚C.

The lentiviral vectors, GV513-ADAMTS16 (Ubi-MCS-CBh-gcGFP-IRES-puromycin) and GV358-BMP2 (Ubi-MCS-3FLAG-SV40-EGFP-IRES-puromycin), and the corresponding control lentiviruses containing the empty vector, CON335 and CON238, respectively, were purchased from Shanghai GeneChem Co., Ltd. Accession numbers for the two genes used in the present study are as follows: ADAMTS16, NM139056; BMP2, NM001200. For lentiviral infection, HepG2 cells were incubated with lentivirus at a MOI of 10 for 16 h, and the stable cell line was selected using 2 μg/ml puromycin for a week, followed by 2 μg/ml puromycin maintenance. The overexpression efficiency of ADAMTS16 and BMP2 were assessed through reverse transcription-quantitative PCR (RT-qPCR).

Transcriptome sequencing and analysis. In total, 40 HCC tissue samples were divided into TB-pos and TB-neg groups by two independent pathologists on the basis of hematoxylin-eosin (HE) staining for transcriptome sequencing, which was conducted by Berry Genomics Co., Ltd. Briefly, using the NEBNext® UltraTM RNA Library Prep Kit for Illumina® (E7770S, New England Biolabs, Inc.), total RNA (≥1 μg) from each sample was used for generating sequencing libraries in-line with the manufacturer's instructions. Oligo (dT) magnetic beads were used to enrich and purify poly A-containing mRNA, followed by random interruption of mRNA into short fragments, which served as templates for random-primed cDNA synthesis performed using reverse transcriptase. Subsequently, purified double-stranded cDNA was subjected to end-repair, A-tailing and adapter ligation. Moreover, AMPure XP beads (Beckman Coulter, Beverly, USA) were used to purify cDNA library fragments for selecting the 250-300 bp cDNA fragments. Lastly, PCR amplification was performed by ABI Q3TMReal-Time PCR System, followed by purification of PCR products using the AMPure XP beads for obtaining the cDNA library.

Following library construction, the Qubit 2.0 Fluorometer (Thermo Fisher Scientific, Inc.) was used to quantify the library before diluting to 1.5 ng/μl. Then, the Agilent 2100 Bioanalyzer was used to assess the library insert size. When the expected insert size was obtained, qPCR was conducted to precisely quantify library effective concentration (>2 nM) for ensuing library quality. After the library quality was confirmed, the Illumina platform was used for sequencing to generate 150 bp paired end reads.

The edgeR software package (version 3.28.1; https://bioconductor.org/packages/release/bioc/html/edgeR.html) (22) in the R/Bioconductor environment (Release 3.6.1) was used for differential expression analysis. To control the false discovery rate, the resulting P-values were adjusted according to the Benjamini and Hochberg's approach (23). Genes with log2 (Fold Change) >1 and Q<0.05 were assigned as differentially expressed. To annotate the function of these DEGs, Gene ontology (GO) enrichment analysis of DEG sets were implemented in topGO (version 2.38.1; http://www.bioconductor.org/packages/release/bioc/html/topGO.html) in the R/Bioconductor environment (Release 3.6.1). GO terms with adjusted P<0.05 were considered as significantly enriched by DEGs.

RT-qPCR. Total RNA from the HepG2 cells was extracted using TRIzol reagent (Ambion; Thermo Fisher Scientific, Inc.). Reverse transcription was conducted using the HiScript

III RT SuperMix for qPCR (+gDNA wiper) (Vazyme Biotech Co., Ltd.) according to the manufacturer's protocol. The reverse transcription reactions were performed at 42˚C for 2 min, followed by 37˚C for 15 min and 85˚C for 5 sec. qPCR was performed using ChamQ Universal SYBR qPCR Master Mix (Vazyme Biotech Co., Ltd.) in a CFX Connect Real-time System (Bio-Rad Laboratories Inc.). GAPDH was employed as the internal reference and the $2^{-\Delta\Delta Cq}$ method was used for quantification (24). Primer sequences for GAPDH, ADAMTS16 and BMP2 were as follows: GAPDH, 5'-CTG ACTTCAACAGCGACACC-3' (forward) and 5'-TGCTGT AGCCAAATTCGTTGT-3' (reverse); ADAMTS16, 5'-CCG GCCGGTACAAATTTTCG-3' (forward) and 5'-AACAGC AGCTCCACAATCAGT-3' (reverse); BMP2, 5'-AGAATG CAAGCAGGTGGGAA-3' (forward) and 5'-TCTTGGTGC AAAGACCTGCT-3' (reverse).

Inverse Matrigel invasion assays. The inverse Matrigel invasion assays were performed as reported previously (25). To evaluate the TB capacity of HepG2 cells, 8-μm pore sized Transwell chambers (Corning, Inc.) were used. Briefly, the Transwell chambers were hydrated using serum-free DMEM medium for 30 min. Then, the Matrigel (BD Biosciences) was added to each chamber and solidified in an incubator at 37˚C for 1 h. Afterwards, the chambers were inverted and the cells ($2x10^5$/well) were seeded onto the upward facing underside of the chamber. Following cell attachment, serum-free DMEM medium was placed in the lower chamber and DMEM medium containing 20% FBS (serving as a chemoattractant) was added to the upper chamber. The cells were allowed to invade through the Matrigel for 3-5 days in a 37˚C incubator. Finally, the 3D reconstruction of cell invasion was obtained through Zeiss 800 laser confocal microscopy. The ratio of the fluorescence values of GFP-positive budding cells/total fluorescence value of all GFP-positive cells x 100% was calculated using Image J software (version 1.8.0) to quantify the invaded cells (TB rate).

Spheroid-based sprouting assays. Spheroid-based sprouting assays were performed as previously described (26), with some optimization. HepG2 spheroids were obtained using the hanging drop method. HepG2 cells were suspended at a density of $1x10^4$ cells/45 μl and then seeded on the lid of 48-well culture plates for 2 days in an incubator at 37˚C. Then, all spheroids were harvested and embedded in Matrigel for 2 days in a 37˚C incubator. Finally, images were captured using a light microscope (OPTIKA).

Immunohistochemistry (IHC). In total, 308 formalin-fixed, paraffin-embedded tissue samples from patients with HCC were used to establish HCC tissue microarrays (TMAs) with a 2.0-mm diameter per core for IHC. In brief, TMAs were dewaxed, hydrated and antigen repaired by EDTA antigen repair buffer (PH 8.0), and the endogenous peroxidase activity was then blocked. TMAs were blocked in goat serum (OriGene Technologies, Inc.) at room temperature for 30 min to block non-specific staining. Primary antibodies were incubated with the TMAs overnight at 4˚C, including ADAMTS16 (1:200; cat. no. DF9173; Affinity Biosciences) and BMP2 (1:200; cat. no. A0231; ABclonal Biotech Co., Ltd.). Subsequently, a horseradish peroxidase-labeled secondary antibody (KIT-5020; Maxim Co., Ltd., Fuzhou, China) was incubated with the TMAs for 30 min at room temperature. Finally, a chromogenic reaction was developed with DAB kit (DAB-0031 (20x); Fuzhou Maixin Biotech Co., Ltd.), followed by counterstaining with hematoxylin (G1120; Beijing Solarbio Science & Technology Co., Ltd.) for 10-30 sec at room temperature. All IHC staining analyses were assessed using a semi-quantitative scoring approach by two senior pathologists. IHC scores were calculated by multiplying staining intensity with the stained area, in which the staining intensity was scored as follows: 0 (no staining), 1 (light yellow staining), 2 (yellow-brown staining) and 3 (brown staining). The staining area was scored as follows: 1 (1-25%), 2 (26-50%), 3 (51-75%) and 4 (76-100%), according to the percentage of stained area in the field of vision. The median IHC score of ADAMTS16 or BMP2 was used as a cut-off to divide the samples into the low expression and high expression groups. 'High' was defined an IHC score higher than the cut-off value, and 'low' was defined as an IHC score lower than or equal the cut-off value.

Statistical analysis. SPSS 25.0 (IBM Corp.) was used for statistical analyses. Differences between two groups were analyzed using the Wilcoxon rank-sum test or unpaired student's t-test. The association of ADAMTS16 and BMP2 expressions with clinicopathological features was analyzed using the chi-square test or Fisher's exact test as appropriate. Kaplan-Meier (KM) curves were generated using the 'survfit' function in the survival package of R software (version 3.5.3), while significant differences in survival were compared using the log-rank test or Cramer-von Mises test as appropriate. Cramer-von Mises test was performed to generate the P-values when KM curves crossed over. $P<0.05$ was considered to indicate a statistically significant difference.

Results

Transcriptome sequencing analysis. A total of 40 surgical HCC specimens were divided into two groups: TB-pos group (n=21) and TB-neg group (n=19), followed by transcriptome sequencing analysis. As shown in the volcano plot in Fig. 1A, 245 DEGs including 95 upregulated DEGs and 150 downregulated DEGs were obtained for the TB-pos group compared with the TB-neg group. GO enrichment analysis was subsequently performed for the 95 upregulated DEGs. The top 20 upregulated biological processes (BPs) are shown in Fig. 1B. The predominant BPs of the upregulated DEGs are associated with embryonic kidney development.

Results of GO (BP) enrichment analysis for downregulated genes are shown in Fig. 1C. It was noted that downregulated genes were mainly involved in immune-related processes, such as immune response, innate immune response and response to type I interferon. Certain studies have illustrated that the downregulated immune-related genes are associated with tumor immune escape (27-29).

The details of BP enrichment of upregulated genes in the GO analysis are provided in Table SI. In the present study, BPs of embryonic kidney development-related processes related to the upregulated genes of HCC with TB was made the focus as this is a novel area. Genes involved in the BPs associated with embryonic kidney development include ADAMTS16, BMP2,

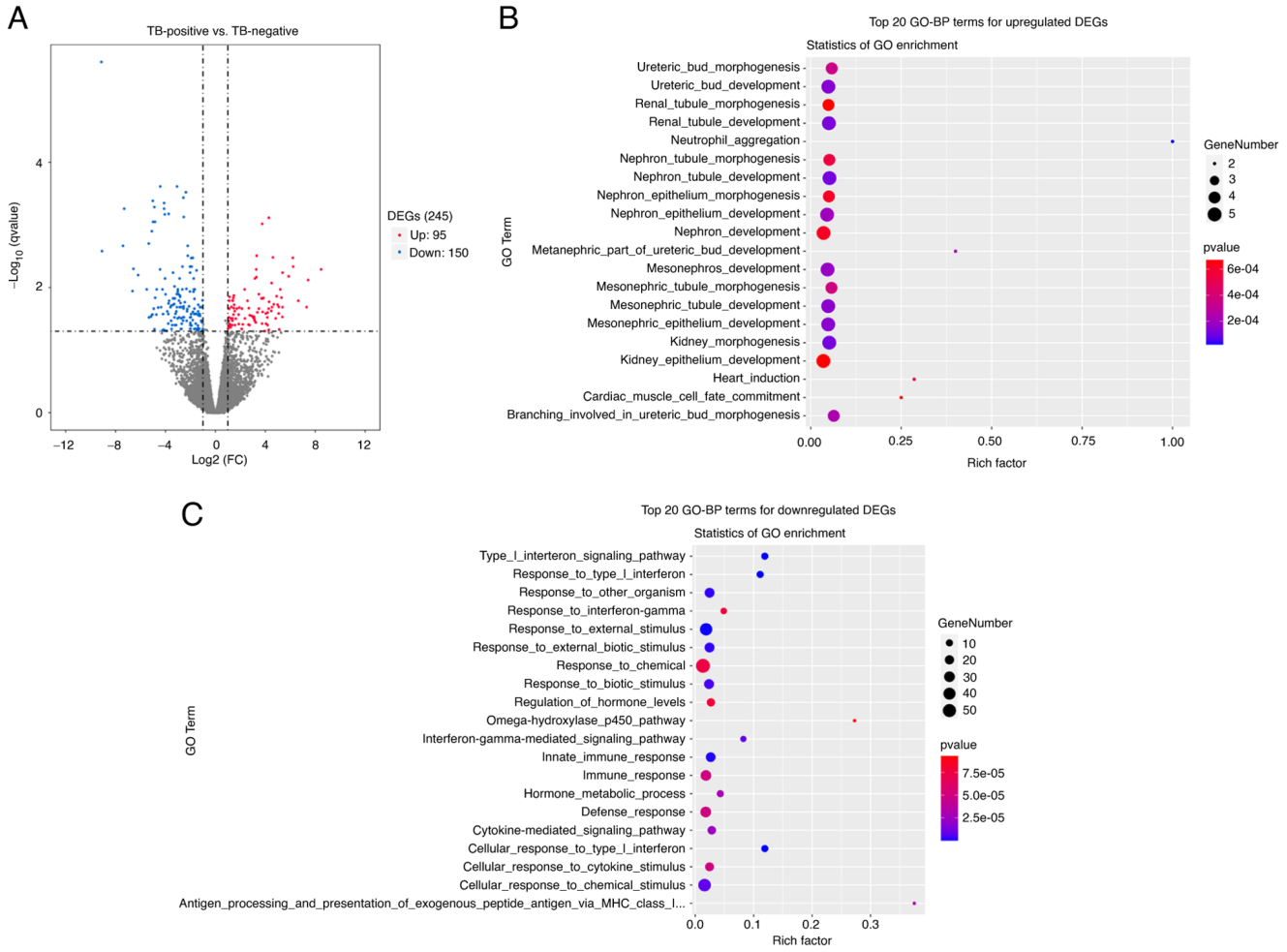

Figure 1. Transcriptome sequencing of hepatocellular carcinoma tissues with different tumor budding statuses. (A) Volcano plot analysis of 95 upregulated DEGs and 150 downregulated DEGs. (B) Top 20 GO-BP terms for upregulated DEGs in TB-positive hepatocellular carcinoma tissues. (C) The top 20 GO-BP terms for downregulated DEGs in TB-positive hepatocellular carcinoma tissues. BPs, biological processes; DEGs, differentially expressed genes; FC, fold change; GO, Gene Ontology.

CALB1, FOXD1 and WT1. Furthermore, we found that there were 4 common upregulated genes in these embryonic kidney development-related processes, including ADAMTS16, BMP2, WT1 and FOXD1. ADAMTS16 and BMP2 were selected for further investigation. In addition, we noted that S100A9 which involved in neutrophil aggregation, was a poor prognosis-related gene. The survival analysis result of S100A9 based on TCGA data showed that the higher expression level of S100A9 was also linked with a worse prognosis of HCC patients (P=0.013) (Fig. S1). It was also reported in the literature that S100A9 expression could potentially serve as an independent prognostic marker for HCC (30).

High ADAMTS16 and BMP2 expression levels are associated with TB in HCC. To identify ADAMTS16 and BMP2 expression profiles within HCC tissues with different TB statuses, IHC staining was performed using TMAs of 308 paraffin-embedded HCC tissues. In addition, the DEGs of the budding cells and cancer center were compared. The statistical analysis results for the IHC staining scores of ADAMTS16 and BMP2 expression are summarized in Tables I and II. As shown in Table I, the staining scores of ADAMTS16 expression in the TB-pos HCC tissues were significantly higher than those in the TB-neg HCC tissues (P=0.005). However, the staining scores of ADAMTS16 expression demonstrated no significant difference between the tumor center and budding cells (P=0.174). As shown in Table II, the staining scores of BMP2 expression were significantly higher in TB-pos group compared with that in TB-neg group (P=0.015), and the significantly higher staining scores in budding cells than in tumor center (P=0.042) were observed. The representative results for IHC staining of ADAMTS16 and BMP2 expressions are illustrated in Fig. 2. These results demonstrated that upregulation of ADAMTS16 and BMP2 expression may be related to TB in HCC. Moreover, BMP2 expression was significantly increased in the budding cells compared with the tumor center.

ADAMTS16 and BMP2 promote the TB of liver cancer in vitro. To explore whether ADAMTS16 and BMP2 play a role in the TB of liver cancer, HepG2 cells with stable ADAMTS16-OE or BMP2-OE were constructed using lentiviral vectors. The overexpression efficiency was assessed through RT-qPCR assays (Fig. S2). Subsequently, the TB ability of HepG2 cells was evaluated using *in vitro* inverse Matrigel invasion and spheroid-based sprouting assays. As shown in Fig. 3A, the ratio of TB in ADAMTS16-OE or BMP2-OE HepG2 cells

Table I. Association between a metalloproteinase domain with thrombospondin motifs 16 expression and TB in hepatocellular carcinoma tissues (n=308).

Group	Median (P25, P75)	Median difference (95% CI)	Two-sample Wilcoxon rank-sum test	
			Z value	P-value
TB		-1.000 (-1.000-0.000)	-2.802	0.005[a]
TB-neg	2 (1, 4)			
TB-pos	3 (1, 6)			
Area		0.000 (-2.000-0.000)	-1.359	0.174
Tumor center	3 (2, 6)			
Budding cells	4 (3, 8)			

[a]P<0.05. neg, negative; pos, positive; TB, tumor budding; P25, lower quartile; P75, upper quartile.

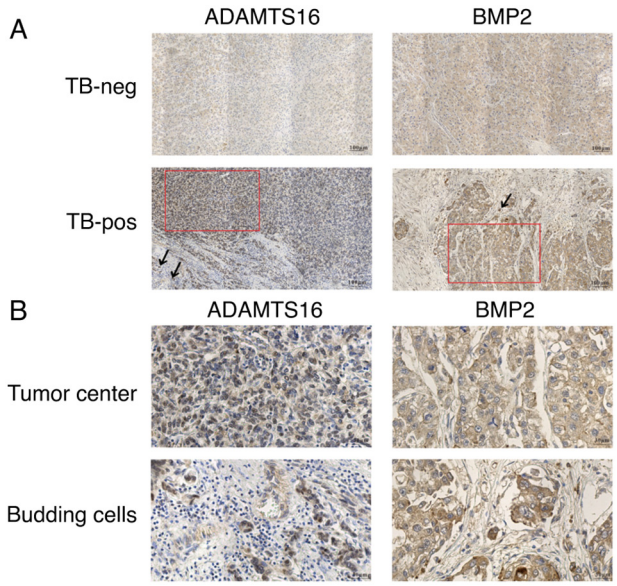

Figure 2. Immunohistochemical analysis of ADAMTS16 and BMP2 in patients with HCC with different TB statuses. (A) Representative IHC staining images of ADAMTS16 and BMP2 in TB-neg and TB-pos HCC tissues (magnification, x100). Red boxes represent the tumor center and black arrows indicate budding tumor cells. (B) Representative IHC images of ADAMTS16 and BMP2 levels in the tumor center and budding cells (magnification, x400), which are magnified views of the areas indicated by the red boxes and black arrows in (A), respectively. ADAMTS16, a metalloproteinase domain with thrombospondin motifs 16; BMP2, bone morphogenetic protein 2; HCC, hepatocellular carcinoma; IHC, immunohistochemistry; neg, negative; pos, positive; TB, tumor budding.

increased significantly relative to their respective controls. Similarly, the results of the spheroid-based sprouting assays demonstrated that ADAMTS16-OE or BMP2-OE in HepG2 cells resulted in more budding cells compared with the control cells (Fig. 3B). These results demonstrated that ADAMTS16 and BMP2 may be involved in the regulation of TB of liver cancer.

Association of ADAMTS16 and BMP2 expression levels with clinicopathological characteristics in HCC. To analyze the association of ADAMTS16 and BMP2 expression levels with HCC clinicopathological characteristics, 266 HCC cases with complete available clinicopathological information for analysis were enrolled. These 266 cases were classified into the low- or high-expression groups by considering the respective median IHC scores for ADAMTS16 and BMP2 expression as the cut-off. The relationship between the clinicopathological characteristics of patients and gene expression was assessed using the chi-square test and Fisher's exact test. Consequently, ADAMTS16 expression was found to be significantly associated with necrosis (P=0.023) and cholestasis (P=0.011) (Table III). As shown in Table IV, BMP2 expression level had a significant association with the Barcelona Clinic Liver Cancer (BCLC) stage (B-C vs. 0-A; P=0.003) and the vessels encapsulating tumor cluster (VETC; P=0.014), which is one of the vessel types in HCC.

Relationship between ADAMTS16 and BMP2 levels and the prognosis of patients with HCC. A total of 242 HCC cases with available follow-up data were enrolled for survival analysis. These 242 HCC cases were divided into two groups (low or high expression) based on the median IHC scores for ADAMTS16 or BMP2. As shown in Fig. 4A and B, the KM survival curves demonstrated that ADAMTS16 expression was statistically significantly associated with overall survival (OS; ADAMTS16, P=0.046) in patients with HCC. In addition, BMP2 expression was not associated with the OS of patients with HCC (BMP2, P=0.59). Subsequently, the survival curves of these two genes were downloaded from the GEPIA database (http://gepia.cancer-pku.cn/detail.php). As shown in Fig. 4C and D, the survival time of patients with HCC with high BMP2 expression significantly decreased compared with that of patients with low BMP2 expression (P=0.0081). ADAMTS16 expression did not differ significantly between the two groups (P=0.24). The GEO database (accession no. GSE76427; http://www.ncbi.nlm.nih.gov/geo/) was also utilized to perform survival analyses comparing expression levels of ADAMTS16 and BMP2 in HCC. The results demonstrated that neither ADAMTS16 (P=0.28) nor BMP2 (P=0.61) expression were associated with the OS time of patients with HCC (Fig. 4E and F). The potential reasons for this discrepancy were elucidated in the discussion.

Table II. Association between bone morphogenetic protein 2 expression and TB in hepatocellular carcinoma tissues (n=308).

Group	Median (P25, P75)	Median difference (95% CI)	Two-sample Wilcoxon rank-sum test	
			Z value	P-value
TB		0.000 (0.000-0.000)	-2.434	0.015[a]
TB-neg	8 (8, 9)			
TB-pos	8 (8, 12)			
Area		0.000 (-2.000-0.000)	-2.038	0.042[a]
Tumor center	8 (8, 12)			
Budding cells	12 (8, 12)			

[a]P<0.05. neg, negative; pos, positive; TB, tumor budding, P25, lower quartile; P75, upper quartile.

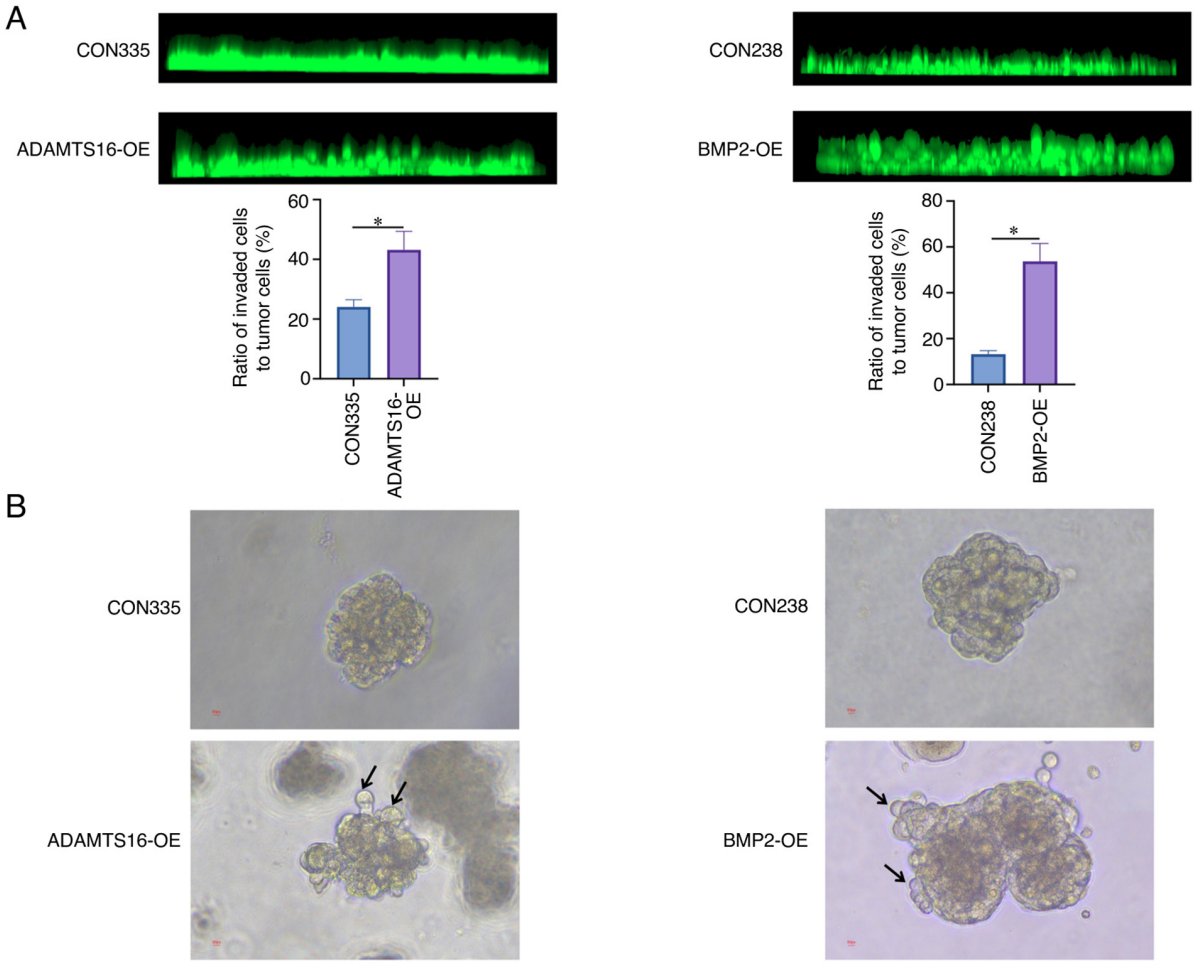

Figure 3. ADAMTS16 and BMP2 promote the TB of liver cancer *in vitro*. HepG2 cells were infected with ADAMTS16-OE lentivirus (GV513-ADAMTS16) or BMP2-OE lentivirus (GV358-BMP2) or corresponding control lentivirus (empty vector), CON335 and CON238, respectively. (A) Representative images (upper panel) and quantification of invaded cells (TB rate) (lower panel) in the inverse Matrigel invasion assays (magnification, x100). The experiments were repeated independently three times. The data were analyzed using an unpaired Student's t-test. Quantitative results are presented as the mean ± SD. *P<0.05. (B) Representative images of the spheroid-based sprouting assays (magnification, x200). Black arrows indicate budding HepG2 cells. ADAMTS16, a metalloproteinase domain with thrombospondin motifs 16; BMP2, bone morphogenetic protein 2; TB, tumor budding; OE, overexpression.

Discussion

TB, a histological phenomenon observed in the tumor invasive edge, has been recognized as the initial stage of cancer invasion and metastasis (31,32). TB has been reported to portend lymphatic/vascular invasion, lymph node metastasis, distant metastasis, failure to respond to neoadjuvant chemoradiotherapy, locoregional relapse and poor survival (6,7,33-37).

Table III. Association between ADAMTS16 expression and the clinicopathological characteristics in patients with hepatocellular carcinoma (n=266).

Clinicopathological characteristics	ADAMTS16 Low, n (n=131)	ADAMTS16 High, n (n=135)	P-value
Age, years			0.848
>60	48	51	
≤60	83	84	
Sex			0.359
Male	105	114	
Female	26	21	
HBV infection			0.193
Positive	116	112	
Negative	15	23	
HCV infection			0.122
Positive	0	4	
Negative	131	131	
AFP serum level, ng/ml			0.407
>400	43	38	
≤400	88	97	
Liver cirrhosis (Yes vs. No)			0.359
Yes	106	103	
No	25	32	
BCLC stage			0.325
B-C	21	16	
0-A	110	119	
Tumor size, cm			0.969
>5	55	57	
≤5	76	78	
Tumor number			0.114
Multiple	12	21	
Single	119	114	
Intrahepatic metastasis			0.114
Yes	12	21	
No	119	114	
Collective invasion			0.693
Yes	9	11	
No	122	124	
Ki-67, %			0.236
>30	31	24	
≤30	100	111	
Necrosis			0.023[a]
Yes	28	15	
No	103	120	
Vessel carcinoma embolus			0.285
Yes	17	12	
No	114	123	
Microtrabecular pattern			0.735
Yes	106	107	
No	25	28	
Macrotrabecular pattern			0.780
Yes	75	75	
No	56	60	
Pseudoglandular pattern			0.130
Yes	23	34	
No	108	101	
Compact pattern			0.865
Yes	53	56	
No	78	79	
Cholestasis			0.011[a]
Yes	17	34	
No	114	101	
Hyaline bodies			0.273
Yes	23	31	
No	108	104	
Steatosis			0.908
Yes	24	24	
No	107	111	
Edmondson grade			0.136
III-IV	46	36	
I-II	85	99	
VETC			0.497
Yes	33	39	
No	98	96	

[a]P<0.05. ADAMTS16, a metalloproteinase domain with thrombospondin motifs 16; HBV, hepatitis B virus; HCV, hepatitis C virus; AFP, α-fetoprotein; BCLC, Barcelona Clinic Liver Cancer; VETC, vessels-encapsulate tumor cluster.

Certain studies have demonstrated an association between TB and low survival rates in numerous types of solid cancers, including nasopharyngeal, lung, pancreatic and esophageal cancer (6-9). However, little is known about the effect of TB on HCC. Moreover, TB can only be definitively determined following surgery and based on detailed pathological and immunohistochemical examinations, thus limiting its role in selecting the therapeutic options for HCC. Therefore, exploring the role of TB in HCC and its molecular mechanisms is crucial for identifying new therapeutic targets for combating HCC.

In the present study, the expression profiles of 40 HCC tissues were analyzed using transcriptome sequencing technology. Functional annotation indicated that upregulated DEGs, obtained by comparing the gene expression of TB-pos and TB-neg HCC tissues, were mainly involved in embryonic kidney development, including nephron tubule development, kidney morphogenesis, renal tubule development and ureteric bud development. With advancements in developmental and cancer biology, numerous studies have suggested that cancer

Table IV. Association between BMP2 expression and the clinicopathological characteristics in patients with hepatocellular carcinoma (n=266).

Clinicopathological characteristics	BMP2 Low, n (n=172)	BMP2 High, n (n=94)	P-value
Age, years			0.290
>60	68	31	
≤60	104	63	
Sex			0.588
Male	140	79	
Female	32	15	
HBV infection			0.105
Positive	143	85	
Negative	29	9	
HCV infection			0.301
Positive	4	0	
Negative	168	94	
AFP serum level, ng/ml			0.508
>400	50	31	
≤400	122	63	
Liver cirrhosis (Yes vs. No)			0.789
Yes	136	73	
No	36	21	
BCLC stage			0.003[a]
B-C	16	21	
0-A	156	73	
Tumor size, cm			0.054
>5	65	47	
≤5	107	47	
Tumor number			0.091
Multiple	17	16	
Single	155	78	
Intrahepatic metastasis			0.091
Yes	17	16	
No	155	78	
Collective invasion			0.604
Yes	14	6	
No	158	88	
Ki-67, %			0.417
>30	33	22	
≤30	139	72	
Necrosis			0.530
Yes	26	17	
No	146	77	
Vessel carcinoma embolus			0.123
Yes	15	14	
No	157	80	
Microtrabecular pattern			0.683
Yes	139	74	
No	33	20	
Macrotrabecular pattern			0.302
Yes	93	57	
No	79	37	
Pseudoglandular pattern			0.964
Yes	37	20	
No	135	74	
Compact pattern			0.511
Yes	73	36	
No	99	58	
Cholestasis			0.750
Yes	32	19	
No	140	75	
Hyaline bodies			0.352
Yes	32	22	
No	140	72	
Steatosis			0.186
Yes	35	13	
No	137	81	
Edmondson grade			0.264
III-IV	49	33	
I-II	123	61	
VETC			0.014[a]
Yes	38	34	
No	134	60	

[a]P<0.05. BMP2, bone morphogenetic protein 2; HBV, hepatitis B virus; HCV, hepatitis C virus; AFP, α-fetoprotein; BCLC, Barcelona Clinic Liver Cancer; VETC, vessels-encapsulate tumor cluster.

invasion and metastasis are similar to normal embryonic development (38-40). Hence, the TB process may be considered to simulate embryonic kidney development. Furthermore, ADAMTS16 and BMP2 were selected from the enriched genes associated with embryonic kidney development for follow-up studies. ADAMTS16 belongs to the ADAMTS family and it has been demonstrated to promote the proliferation and invasion of gastric cancer (41) and esophageal cancer (15) cells. However, to the best of our knowledge, the function of ADAMTS16 has not yet been studied in HCC. BMP2, which belongs to the transforming growth factor-β superfamily, participates in different cancer occurrence and development processes (17-19). Certain studies have indicated that BMP2 may enhance HCC cell growth, invasion and migration (20,21). However, to the best of our knowledge, no study has discussed the relationship between BMP2 and TB in HCC.

The IHC results in the present study indicated an upregulation of ADAMTS16 and BMP2 expression in TB-pos HCC tissues compared with TB-neg HCC tissues. BMP2 expression

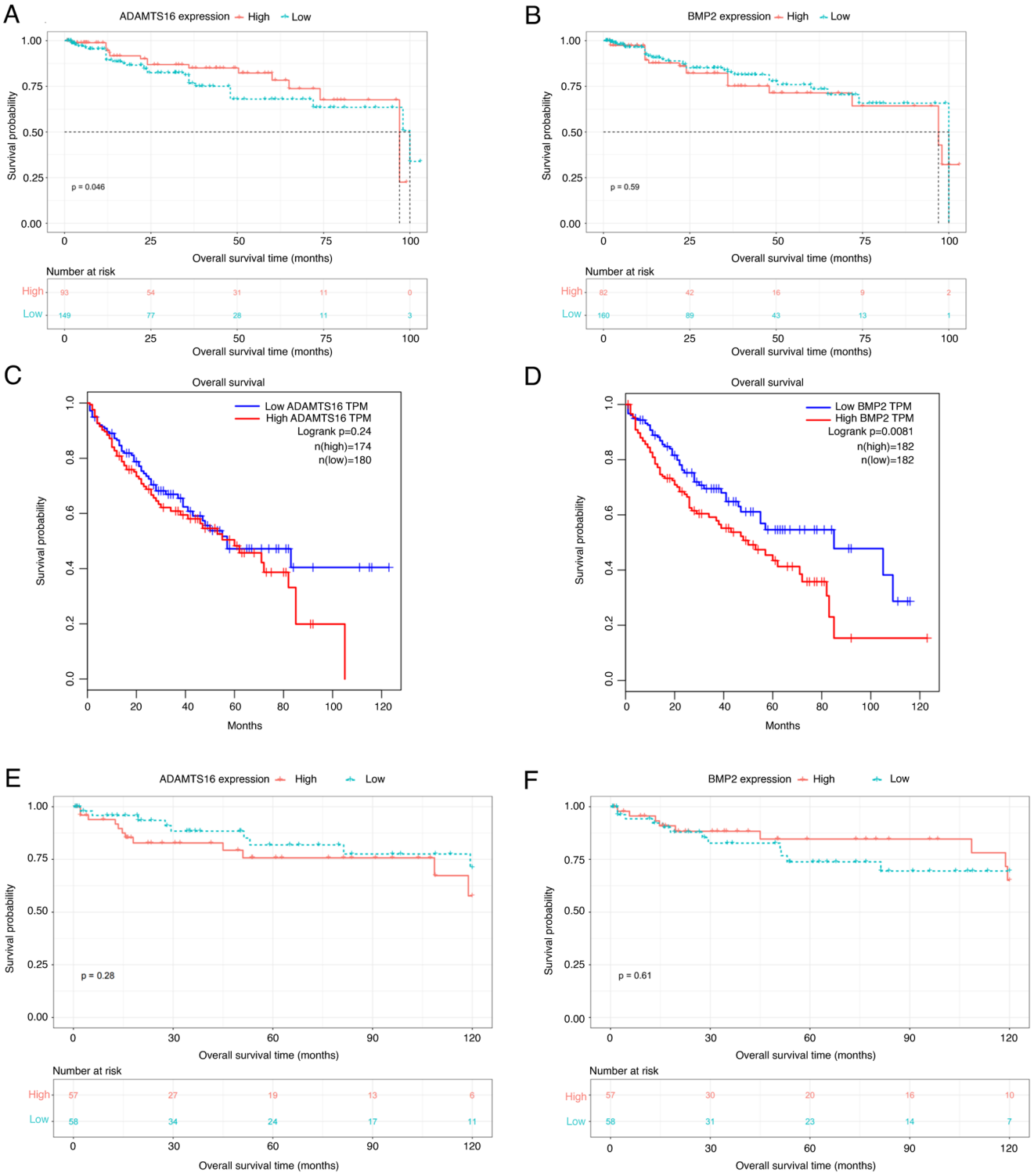

Figure 4. KM survival curves for ADAMTS16 and BMP2 expression. (A) KM curves (Cramer-von Mises test) for the overall survival of patients with HCC in the ADAMTS16 high-expression group (n=93) vs. the ADAMTS16 low-expression group (n=149). (B) KM curves (Cramer-von Mises test) for overall survival of patients with HCC in the BMP2 high-expression group (n=82) vs. the BMP2 low-expression group (n=160). (C) KM curves (log-rank test) for overall survival of patients with HCC with high/low ADAMTS16 expression using The Cancer Genome Atlas data. (D) KM curves (log-rank test) for overall survival of patients with HCC with high/low BMP2 expression using The Cancer Genome Atlas data. (E) KM curves (log-rank test) for overall survival of patients with HCC with high/low ADAMTS16 expression using the GSE76427 dataset. (F) KM curves (Cramer-von Mises test) for overall survival of patients with HCC with high/low BMP2 expression. ADAMTS16, a metalloproteinase domain with thrombospondin motifs 16; BMP2, bone morphogenetic protein 2; HCC, hepatocellular carcinoma; KM, Kaplan-Meier; TPM, transcripts per million.

in budding cells was also increased compared with that in the tumor center. Moreover, through the inverse Matrigel invasion and spheroid-based sprouting assays, the present study revealed that ADAMTS16 and BMP2 may regulate the TB process of liver cancer. Therefore, we hypothesize that these two genes may be associated with the malignant progression of

liver cancer. Furthermore, the association of ADAMTS16 and BMP2 expression with clinicopathological characteristics of patients with HCC was analyzed, and an association between ADAMTS16 expression and necrosis and cholestasis was confirmed in. In addition, BMP2 expression was significantly associated with the BCLC stage and VETC.

It is well known that rapidly growing tumor cells, which represent an important malignant behavior of tumors, require an adequate supply of oxygen and nutrients, and the blood supply cannot meet this need of rapid tumor growth, eventually resulting in tumor necrosis (42). Therefore, the significant association between ADAMTS16 and necrosis in HCC observed in the present study may be caused by the ability of ADAMTS16 to promote tumor malignant progression of HCC. To the best of our knowledge, no study has reported the association of ADAMTS family members with cholestasis. However, a close relative of the ADAMTS family, ADAM17, has been reported to be related to cholestasis (43). Increased ADAM17 expression was found in patients with two important cholestatic liver diseases, including primary biliary cholangitis and primary sclerosing cholangitis (43). Given the functional similarity of these two genes, the result regarding the association of ADAMTS16 with cholestasis in HCC is reasonable and reliable.

As for BMP2, in the present study, patients with BCLC stage B-C had significantly higher BMP2 expression levels than patients with BCLC stage 0-A, suggesting the involvement of BMP2 in the progression and metastasis of HCC. Previous studies have demonstrated that BMP2 may promote HCC cell proliferation and invasion, thereby promoting malignant progression of HCC (20,21,44). As such, the results of the present study are in accordance with previously reported results. Certain studies have also demonstrated that BMP2 promotes angiogenesis of solid tumors, including HCC (45,46). In addition, VETC, a novel vascular pattern distinct from microvascular invasion, has become a powerful predictor of aggressive HCC (47). To the best of our knowledge, the present study is the first to report that BMP2 is significantly associated with VETC in HCC, which may explain the mechanism of this specific angiogenesis pattern in HCC. Tumor malignancy is closely associated with the invasiveness and metastasis of tumor which depends upon EMT (48,49). And TB is considered to be an EMT-like process (10). It has been documented that ADAMTS16 may promote cell migration and invasion through the NF-κB pathway (41). In addition, BMP2 also enhances the migration, invasion and EMT of tumor cells through the m-TOR signaling pathway (45,50). Hence, it is speculated that a contributing mechanism to TB in HCC may involve the m-TOR and/or NF-κB pathways.

The overall survival analysis of 242 patients with HCC indicated that ADAMTS16 expression was associated with HCC prognosis whereas BMP2 expression was not associated with HCC prognosis. In addition, the survival data obtained in the present study is inconsistent with the results predicted using the GSE76427 dataset and the results predicted using GEPIA, which is a The Cancer Genome Atlas (TCGA)-based online tool. The results of the GEPIA analysis demonstrated that BMP2 upregulation was significantly associated with poor OS. The results of the GSE76427 dataset showed that neither ADAMTS16 expression nor BMP2 expression was associated with HCC prognosis. The possible reasons for this discrepancy are as follows: Firstly, sample size varied widely across these three cohorts. which may cause the inconsistent results. And compared with the large sample size within the TCGA cohort, the retrospective cohort of the present study and the GSE76427 cohort have relatively small sample sizes. Secondly, the sources of the tumor samples in the three cohorts were different. The majority of patients from TCGA database are white. In GSE76427 cohort, all of the patients were derived from Singapore. And our study is based on data collected from a single center (Affiliated Hospital of Jining Medical University, China). Thirdly, as patient characteristics, surgical skills and treatment regimens are different among countries, the final outcome of patients with HCC could be affected. The absence of animal models of HCC is also a limitation of this study, animal models of HCC will be constructed for further study validation in the future.

Regardless of these limitations, to the best of our knowledge, the present study was the first to investigate the TB-related molecular mechanism in HCC. The findings of the present study provide evidence for mechanism studies of TB. Moreover, the present study provides a basis for the potential application of ADAMTS16 and BMP2 as predictive diagnosis markers and treatment targets for HCC.

Acknowledgements

Not applicable.

Funding

The present study was funded by the National Natural Science Foundation of China (grant no. 81972629), the Taishan Scholars Program of Shandong Province (grant no. tsqn201909193), the Shandong Youth Innovation and Technology program (grant no. 2020KJL003), the Jining Research and Development Program (grant nos. 2021YXNS065 and 2021YXNS075), and the Research Fund for Lin He Academician New Medicine (grant no. JYHL2021FMS12).

Availability of data and materials

The RNA-Seq datasets generated and/or analyzed during the current study are available in the GEO repository, the accession number is GSE227335. All other data generated or analyzed during this study are included in this published article.

Authors' contributions

DJ performed the experiments, data analysis and collection of clinical specimens, and drafted the manuscript. SX assisted with the data analysis and reverse transcription-quantitative PCR. CZ performed the bioinformatics analysis of the GEO database. CZ, CH and LL contributed to the analysis and interpretation of the data. MZ and HW contributed to the acquisition and interpretation of the data. DY and YL conceived and designed the study. YL revised the manuscript. DJ and SX confirm the authenticity of all the raw data. All authors have read and approved the final manuscript.

Ethics approval and consent to participate

Written informed consent was obtained from all patients. The study was approved by The Ethics Committee of the Affiliated Hospital of Jining Medical University (ethical approval no. 2021C145; Jining, China).

Patient consent for publication

Not applicable.

Competing interests

The authors declare that they have no competing interests.

References

1. Sung H, Ferlay J, Siegel RL, Laversanne M, Soerjomataram I, Jemal A and Bray F: Global cancer statistics 2020: GLOBOCAN estimates of incidence and mortality worldwide for 36 cancers in 185 countries. CA Cancer J Clin 71: 209-249, 2021.
2. Bray F, Ferlay J, Soerjomataram I, Siegel RL, Torre LA and Jemal A: Global cancer statistics 2018: GLOBOCAN estimates of incidence and mortality worldwide for 36 cancers in 185 countries. CA Cancer J Clin 68: 394-424, 2018.
3. Yang JD, Hainaut P, Gores GJ, Amadou A, Plymoth A and Roberts LR: A global view of hepatocellular carcinoma: Trends, risk, prevention and management. Nat Rev Gastroenterol Hepatol 16: 589-604, 2019.
4. Turajlic S and Swanton C: Metastasis as an evolutionary process. Science 352: 169-175, 2016.
5. Hase K, Shatney C, Johnson D, Trollope M and Vierra M: Prognostic value of tumor 'budding' in patients with colorectal cancer. Dis Colon Rectum 36: 627-635, 1993.
6. Koike M, Kodera Y, Itoh Y, Nakayama G, Fujiwara M, Hamajima N and Nakao A: Multivariate analysis of the pathologic features of esophageal squamous cell cancer: Tumor budding is a significant independent prognostic factor. Ann Surg Oncol 15: 1977-1982, 2008.
7. Luo WR, Gao F, Li SY and Yao KT: Tumour budding and the expression of cancer stem cell marker aldehyde dehydrogenase 1 in nasopharyngeal carcinoma. Histopathology 61: 1072-1081, 2012.
8. Masuda R, Kijima H, Imamura N, Aruga N, Nakamura Y, Masuda D, Takeichi H, Kato N, Nakagawa T, Tanaka M, *et al*: Tumor budding is a significant indicator of a poor prognosis in lung squamous cell carcinoma patients. Mol Med Rep 6: 937-943, 2012.
9. Karamitopoulou E, Zlobec I, Born D, Kondi-Pafiti A, Lykoudis P, Mellou A, Gennatas K, Gloor B and Lugli A: Tumour budding is a strong and independent prognostic factor in pancreatic cancer. Eur J Cancer 49: 1032-1039, 2013.
10. Grigore AD, Jolly MK, Jia D, Farach-Carson MC and Levine H: Tumor budding: The name is EMT. Partial EMT. J Clin Med 5: 51, 2016.
11. De Smedt L, Palmans S, Andel D, Govaere O, Boeckx B, Smeets D, Galle E, Wouters J, Barras D, Suffiotti M, *et al*: Expression profiling of budding cells in colorectal cancer reveals an EMT-like phenotype and molecular subtype switching. Br J Cancer 116: 58-65, 2017.
12. Kairaluoma V, Kemi N, Pohjanen VM, Saarnio J and Helminen O: Tumour budding and tumour-stroma ratio in hepatocellular carcinoma. Br J Cancer 123: 38-45, 2020.
13. Wei L, Delin Z, Kefei Y, Hong W, Jiwei H and Yange Z: A classification based on tumor budding and immune score for patients with hepatocellular carcinoma. Oncoimmunology 9: 1672495, 2019.
14. Zhang D, Qian C, Wei H and Qian X: Identification of the prognostic value of tumor microenvironment-related genes in esophageal squamous cell carcinoma. Front Mol Biosci 7: 599475, 2020.
15. Sakamoto N, Oue N, Noguchi T, Sentani K, Anami K, Sanada Y, Yoshida K and Yasui W: Serial analysis of gene expression of esophageal squamous cell carcinoma: ADAMTS16 is upregulated in esophageal squamous cell carcinoma. Cancer Sci 101: 1038-1044, 2010.
16. Mersakova S, Janikova K, Kalman M, Marcinek J, Grendar M, Vojtko M, Kycina R, Pindura M, Janik J, Mikolajcik P, *et al*: Cancer stem cell marker expression and methylation status in patients with colorectal cancer. Oncol Lett 24: 231, 2022.
17. Raida M, Clement JH, Ameri K, Han C, Leek RD and Harris AL: Expression of bone morphogenetic protein 2 in breast cancer cells inhibits hypoxic cell death. Int J Oncol 26: 1465-1470, 2005.
18. Yang S, Pham LK, Liao CP, Frenkel B, Reddi AH and Roy-Burman P: A novel bone morphogenetic protein signaling in heterotypic cell interactions in prostate cancer. Cancer Res 68: 198-205, 2008.
19. Hsu YL, Huang MS, Yang CJ, Hung JY, Wu LY and Kuo PL: Lung tumor-associated osteoblast-derived bone morphogenetic protein-2 increased epithelial-to-mesenchymal transition of cancer by Runx2/Snail signaling pathway. J Biol Chem 286: 37335-37346, 2011.
20. Wu G, Huang F, Chen Y, Zhuang Y, Huang Y and Xie Y: High levels of BMP2 promote liver cancer growth via the activation of myeloid-derived suppressor cells. Front Oncol 10: 194, 2020.
21. Liu Z, Sun J, Wang X and Cao Z: MicroRNA-129-5p promotes proliferation and metastasis of hepatocellular carcinoma by regulating the BMP2 gene. Exp Ther Med 21: 257, 2021.
22. Robinson MD, McCarthy DJ and Smyth GK: edgeR: A bioconductor package for differential expression analysis of digital gene expression data. Bioinformatics 26: 139-140, 2010.
23. Benjamini Y and Hochberg Y: Controlling the false discovery rate-a practical and powerful approach to multiple testing. J Roy Statist Soc B 57: 289-300, 1995.
24. Livak KJ and Schmittgen TD: Analysis of relative gene expression data using real-time quantitative PCR and the 2(-Delta Delta C(T)) method. Methods 25: 402-408, 2001.
25. Scott RW, Crighton D and Olson MF: Modeling and imaging 3-dimensional collective cell invasion. J Vis Exp: 3525, 2011.
26. Pfisterer L and Korff T: Spheroid-based in vitro angiogenesis model. Methods Mol Biol 1430: 167-177, 2016.
27. Muenst S, Läubli H, Soysal SD, Zippelius A, Tzankov A and Hoeller S: The immune system and cancer evasion strategies: Therapeutic concepts. J Intern Med 279: 541-562, 2016.
28. Aust S, Felix S, Auer K, Bachmayr-Heyda A, Kenner L, Dekan S, Meier SM, Gerner C, Grimm C and Pils D: Absence of PD-L1 on tumor cells is associated with reduced MHC I expression and PD-L1 expression increases in recurrent serous ovarian cancer. Sci Rep 7: 42929, 2017.
29. Baloche V, Rivière J, Tran TBT, Gelin A, Bawa O, Signolle N, Diop MBK, Dessen P, Beq S, David M and Busson P: Serial transplantation unmasks galectin-9 contribution to tumor immune escape in the MB49 murine model. Sci Rep 11: 5227, 2021.
30. Liao J, Li JZ, Xu J, Xu Y, Wen WP, Zheng L and Li L: High $S100A9^{+}$ cell density predicts a poor prognosis in hepatocellular carcinoma patients after curative resection. Aging (Albany NY) 13: 16367-16380, 2021.
31. Liang F, Cao W, Wang Y, Li L, Zhang G and Wang Z: The prognostic value of tumor budding in invasive breast cancer. Pathol Res Pract 209: 269-275, 2013.
32. Prall F: Tumour budding in colorectal carcinoma. Histopathology 50: 151-162, 2007.
33. Morodomi T, Isomoto H, Shirouzu K, Kakegawa K, Irie K and Morimatsu M: An index for estimating the probability of lymph node metastasis in rectal cancers. Lymph node metastasis and the histopathology of actively invasive regions of cancer. Cancer 63: 539-543, 1989.
34. Ueno H, Murphy J, Jass JR, Mochizuki H and Talbot IC: Tumour 'budding' as an index to estimate the potential of aggressiveness in rectal cancer. Histopathology 40: 127-132, 2002.
35. Mitrovic B, Schaeffer DF, Riddell RH and Kirsch R: Tumor budding in colorectal carcinoma: Time to take notice. Mod Pathol 25: 1315-1325, 2012.
36. Satoh K, Nimura S, Aoki M, Hamasaki M, Koga K, Iwasaki H, Yamashita Y, Kataoka H and Nabeshima K: Tumor budding in colorectal carcinoma assessed by cytokeratin immunostaining and budding areas: Possible involvement of c-Met. Cancer Sci 105: 1487-1495, 2014.
37. Rogers AC, Gibbons D, Hanly AM, Hyland JM, O'Connell PR, Winter DC and Sheahan K: Prognostic significance of tumor budding in rectal cancer biopsies before neoadjuvant therapy. Mod Pathol 27: 156-162, 2014.
38. Li A and Machesky LM: Melanoblasts on the move: Rac1 sets the pace. Small GTPases 3: 115-119, 2012.
39. Gupta S and Maitra A: EMT: Matter of life or death? Cell 164: 840-842, 2016.

40. Yu M, Bardia A, Wittner BS, Stott SL, Smas ME, Ting DT, Isakoff SJ, Ciciliano JC, Wells MN, Shah AM, *et al*: Circulating breast tumor cells exhibit dynamic changes in epithelial and mesenchymal composition. Science 339: 580-584, 2013.
41. Li T, Zhou J, Jiang Y, Zhao Y, Huang J, Li W, Huang Z, Chen Z, Tang X, Chen H and Yang Z: The novel protein ADAMTS16 promotes gastric carcinogenesis by targeting IFI27 through the NF-κb signaling pathway. Int J Mol Sci 23: 11022, 2022.
42. Wu CX, Lin GS, Lin ZX, Zhang JD, Chen L, Liu SY, Tang WL, Qiu XX and Zhou CF: Peritumoral edema on magnetic resonance imaging predicts a poor clinical outcome in malignant glioma. Oncol Lett 10: 2769-2776, 2015.
43. Almishri W, Swain LA, D'Mello C, Le TS, Urbanski SJ and Nguyen HH: ADAM metalloproteinase domain 17 regulates cholestasis-associated liver injury and sickness behavior development in mice. Front Immunol 12: 779119, 2022.
44. Guo J, Guo M and Zheng J: Inhibition of BONE MORPHOGENETIC PROtein 2 suppresses the stemness maintenance of cancer stem cells in hepatocellular carcinoma via the MAPK/ERK pathway. Cancer Manag Res 13: 773-785, 2021.
45. Zuo WH, Zeng P, Chen X, Lu YJ, Li A and Wu JB: Promotive effects of bone morphogenetic protein 2 on angiogenesis in hepatocarcinoma via multiple signal pathways. Sci Rep 6: 37499, 2016.
46. Raida M, Clement JH, Leek RD, Ameri K, Bicknell R, Niederwieser D and Harris AL: Bone morphogenetic protein 2 (BMP-2) and induction of tumor angiogenesis. J Cancer Res Clin Oncol 131: 741-750, 2005.
47. Renne SL, Woo HY, Allegra S, Rudini N, Yano H, Donadon M, Viganò L, Akiba J, Lee HS, Rhee H, *et al*: Vessels encapsulating tumor clusters (VETC) is a powerful predictor of aggressive hepatocellular carcinoma. Hepatology 71: 183-195, 2020.
48. Rodriguez MI, Peralta-Leal A, O'Valle F, Rodriguez-Vargas JM, Gonzalez-Flores A, Majuelos-Melguizo J, López L, Serrano S, de Herreros AG, Rodríguez-Manzaneque JC, *et al*: PARP-1 regulates metastatic melanoma through modulation of vimentin-induced malignant transformation. PLoS Genet 9: e1003531, 2013.
49. Mani SA, Guo W, Liao MJ, Eaton EN, Ayyanan A, Zhou AY, Brooks M, Reinhard F, Zhang CC, Shipitsin M, *et al*: The epithelial-mesenchymal transition generates cells with properties of stem cells. Cell 133: 704-715, 2008.
50. Wang MH, Zhou XM, Zhang MY, Shi L, Xiao RW, Zeng LS, Yang XZ, Zheng XFS, Wang HY and Mai SJ: BMP2 promotes proliferation and invasion of nasopharyngeal carcinoma cells via mTORC1 pathway. Aging (Albany NY) 9: 1326-1340, 2017.